Single Pile Versus Pile Group Lateral Response Under Asymmetric Cyclic Loading

S. Giannakos, N. Gerolymos, G. Gazetas
National Technical University of Athens, Athens,Greece

ABSTRACT: To gain insight into the inelastic behavior of piles, the response of a vertical pile embedded in a dry dense sand and subjected to cyclic lateral loading was studied experimentally in centrifuge tests conducted in Laboratoire Central des Ponts et Chaussees, in Nantes, France. A three-dimensional finite element analysis with the use of a new constitutive model for the cyclic behavior of sand was performed in order to capture the cyclic response of the single pile. Performance measure parameters were introduced to evaluate the overall response of the pile-soil system indicating that the proposed model is suitable for the prediction of the lateral response of a pile under cyclic loading and the domination of the mechanism of "system densification" upon soil densification in cyclic loading. The response of an 1x2 pile group under cyclic lateral loading is also investigated showing that the model is capable of representing the shadow effect of the pile group.

1 CENTRIFUGE LATERAL CYCLIC LOAD PILE EXPERIMENTS

Three centrifuge tests on a single pile subjected to cyclic horizontal loading were performed by Rosquoët et al (2004) at Laboratoire Central des Ponts et Chaussées (LCPC). The centrifuge models were 1/40 in scale and involved pile head loading with three different force time histories. The loading time histories were: i) 12 cycles from 960 kN to 480 kN (test P32) ii) 12 cycles from 960 kN to 0 kN (test P344) iii) 6 cycles from 960 kN to -960 kN (test P330). The experimental set up and the loading time histories (in prototype scale) are portrayed in Figure 1.

The cyclic lateral load tests were conducted on vertical friction pile placed in a sand mass of uniform density. The Fontainebleau sand centrifuge specimens were prepared by the air sand-raining process into a rectangular container (80 cm wide by 120 cm long by 36 cm deep), with the use of a special automatic hopper developed at LCPC (Garnier, 2002). The desired density of the dry sand was obtained by varying three parameters: a) the flow of sand (opening of the hopper), b) the automatically maintained drop height, and c) the scanning rate. Laboratory results from drained and undrained torsional and direct shear tests on Fontainebleau sand reconstituted specimens indicated mean values of peak and critical-state angles of $\varphi_p = 41.8^o$ and $\varphi_{cv} = 33^o$, respectively. Figure 1 depicts the idealized small strain shear modulus G_o used. Evidently, in this dense sand the pile used may be considered as flexible. The model pile at scale 1/40 is a hollow aluminum cylinder of 18 mm external diameter, 3 mm wall thickness, and 365 mm length. The flexural stiffness of the pile is 0.197 kN m^2 and the elastic limit stress of the aluminum is 245 MPa. The centrifuge tests were carried out at 40 g.

The instrumentation included two displacement sensors, located at the section of the pile above the ground surface, and 20 pairs of strain gauges, positioned along the length of the pile so that the bending moment profile M(z) could be measured during the tests. The resultant earth pressure p = p(z), per unit length along the pile, was obtained by double differentiation of M(z)

as established by Matlock and Reese (Reese and Van Impe, 2001). The strain gauges were spaced at 0.6 m in prototype scale starting from the ground level to the pile tip. This single pile was driven into the sand at 1 g before rotating of the centrifuge. In flight, the single pile was subjected quasi-statically to horizontal cyclic loading through a servo-jack connected to the pile with a cable. With such a configuration the pile head is not submitted to any parasitic bending moment. The test results were obtained in the form of horizontal force-displacement time histories at the head of the pile, as well as of bending moment along the pile.
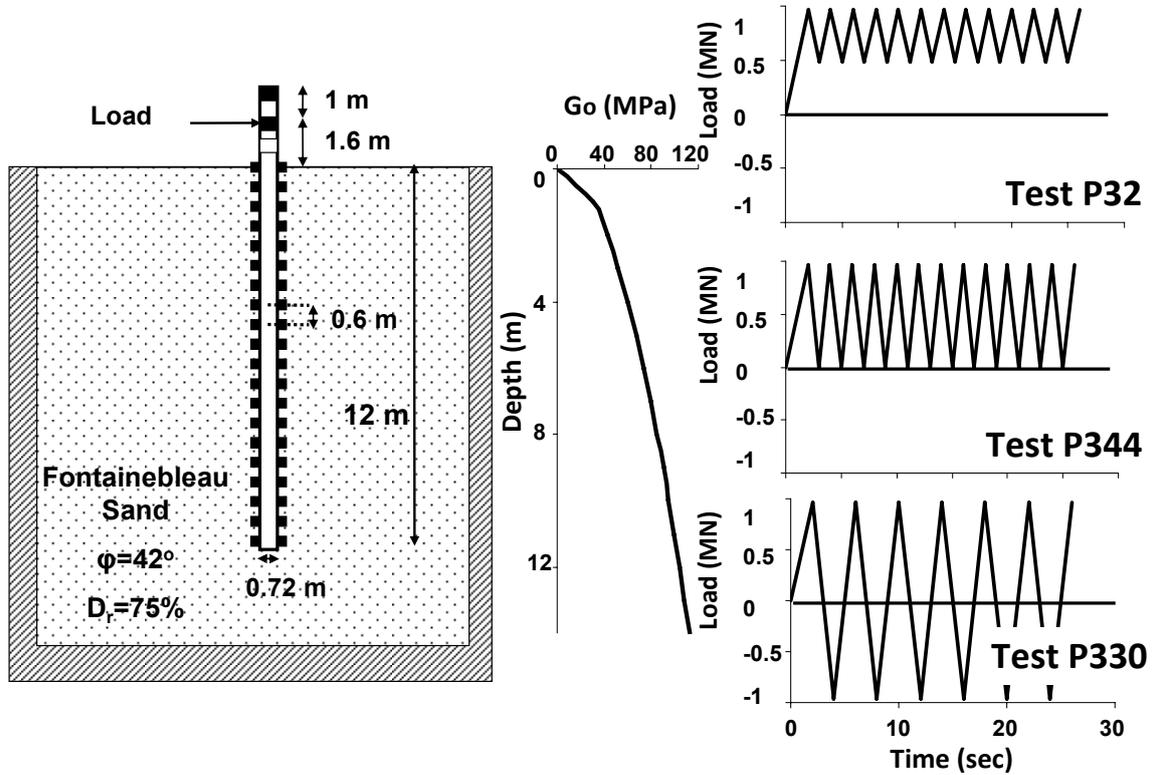
Figure 1. Experimental setup of the centrifuge tests conducted in LCPC (Rosquoët et al, 2004) and load time histories of the three tests (P32, P344 and P330). All dimensions refer to the modeled prototype
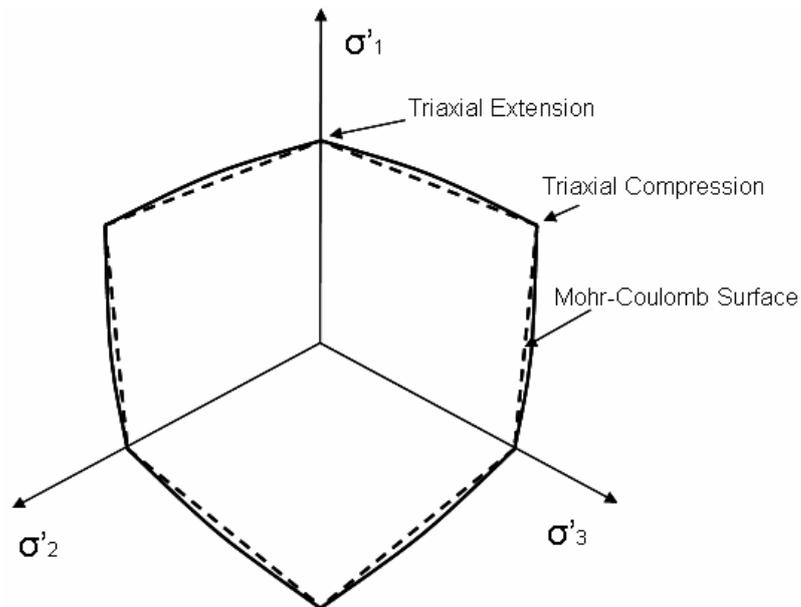
Figure 2. Shape of yield criterion of the proposed constitutive model

2 FINITE ELEMENT MODELING

The above mentioned centrifuge tests were modeled numerically in 3D using the finite element code ABAQUS. The pile is assumed to be linear elastic while the cyclic soil behavior is described via a nonlinear constitutive law with kinematic hardening law and associated plastic flow rule. Approximately 43000 elements were used for each analysis. The soil is modeled with 8-node brick elements while the pile is modeled with 3D beam elements placed at its center and connected with appropriate kinematic restraints with the nodes at the perimeter of the pile in order to model the complete geometry of the pile. The solid elements inside the perimeter of the pile have no stiffness. In this way, each pile section behaves as a rigid disc: rotation is allowed on the condition that the disc remains always perpendicular to the beam axis, but stretching cannot occur.

3 CONSTITUTIVE SOIL MODEL

Soil behavior is modeled through a constitutive model with nonlinear kinematic hardening and associated plastic flow rule. The evolution law of the model consists of two components: a nonlinear kinematic hardening component, which describes the translation of the yield surface in the stress space (defined through the back-stress α), and an isotropic hardening component, which defines the size of the yield surface $\sigma 0$ at zero plastic deformation. The kinematic hardening component is defined as an additive combination of a purely kinematic term (linear Ziegler hardening law) and a relaxation term (the recall term), which introduces the nonlinearity. The model incorporates two hardening parameters C and γ that define the maximum transition of the yield surface, and the rate of transition, respectively. A user subroutine is imported in ABAQUS, which relates the model parameters to the principal stresses and the Lode angle at every loading step. Incorporating the Lode angle effect allows for significant accuracy in three-dimensional shear response environments. The yield surface of the proposed constitutive model is determined to fit the Mohr-Coulomb failure response in a triaxial loading test for both compression and extension conditions assuming linear interpolation for the intermediate stress states. For this reason, the parameter k is introduced which is a function of Lode angle and takes values from 0 to 1. $k=0$ corresponds to pure triaxial extension conditions and $k=1$ to pure triaxial compression conditions. In summary, the constitutive model parameters are calibrated to match the Coulomb failure criterion on the principal stresses plane for every apex of the hexagon with the smooth envelope of Figure 2.

The distribution of Young's modulus varies parabolically with depth according to:

$$C = E = E_0 \left(\frac{\sigma_v}{100} \right)^m \tag{1}$$

where E_0 is the reference Young's modulus, σ_v the vertical stress and m a parameter that defines the distribution of E with depth. E_0 is equal to 192000 kPa and m is equal to 0.5 according to the calibration performed by Gerolymos et al (2009). The hardening parameter γ, which is a function of the internal friction angle, was calibrated to correspond to a critical-state friction angle $\varphi_{cv} = 33^o$. The constitutive model parameters E_0, m and γ were calibrated only to predict the recorded "force – displacement" curve at the head of the pile from the strain gauges for the 12 cycles of loading of test P32.

4 NUMERICAL SIMULATION

The model is then used to simulate test P344 where the single pile is subjected to one-way cyclic load with maximum horizontal force 960 kN and minimum horizontal force 0 kN. Subsequently it is applied to predict the response of an 1x2 pile group subjected to the same average horizontal cyclic loading. It should be noted that the applied loads always stay in the domain of service loads. Bending moment, shear force and soil reaction profiles were compared, but due to lack of space, only the results for the bending moments are presented herein.

4.1 *Simulation of single pile*

The computed force-displacement curve at the pile head is compared to the experimental data in Figure 3 for the 12 cycles of loading. In one way cyclic loading, the pile displacement increases as the number of cycles increases. In this figure it is observed that the model is capable of predicting the plastic shakedown response of the pile. This plastic shakedown response is the resultant of the following two mechanisms: (a) Soil densification due to the reduction of voids, and (b) "System densification" due to the gradual extension of the resisting soil mass, towards greater depths with cyclic loading. Only the second mechanism is captured by the proposed model. Despite the small discrepancy in the residual displacement at the pivot point of each unloading phase, the comparison is quite satisfactory.
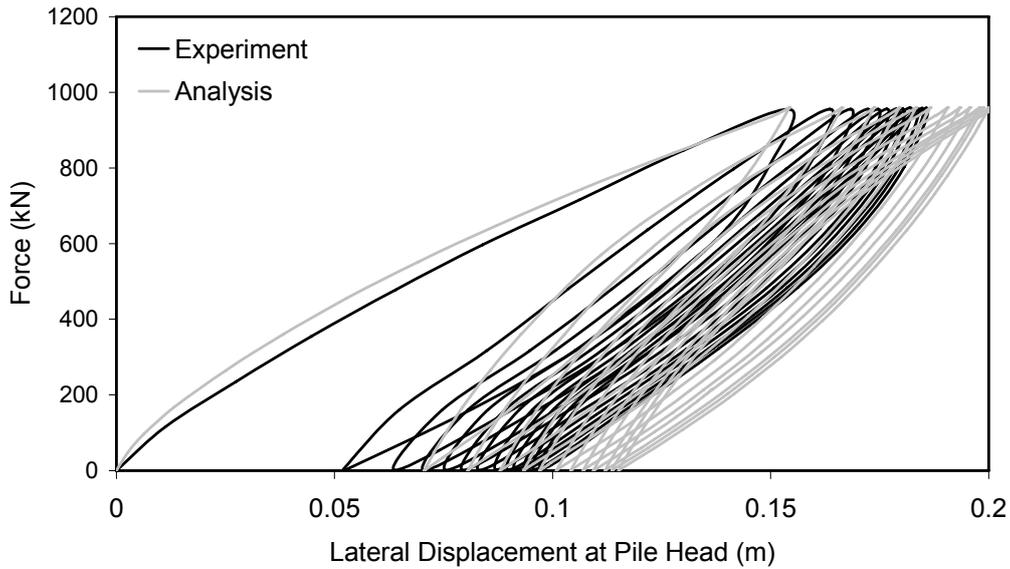
Figure 3. Experimental and Computed Force – Displacement curve at pile head for single pile
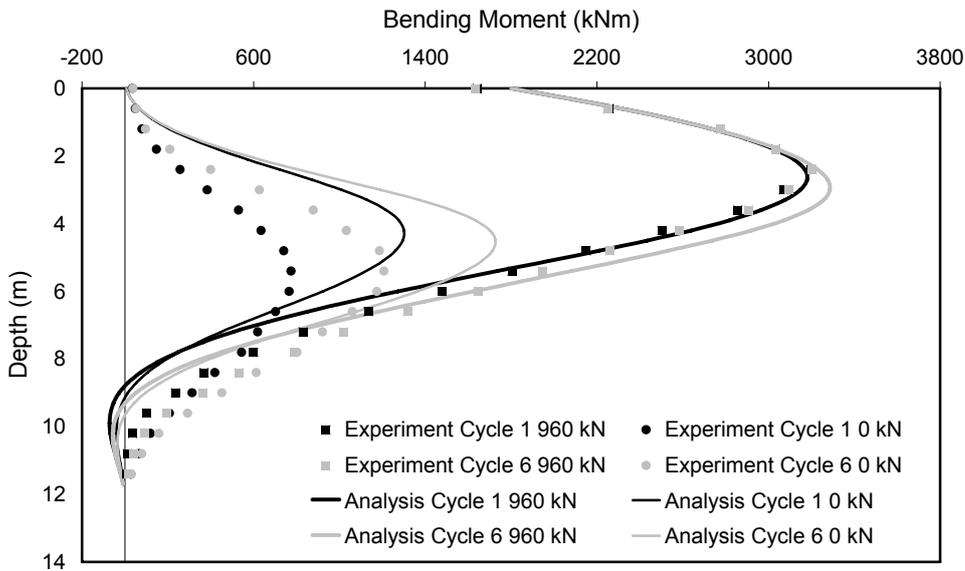
Figure 4. Comparison of computed and recorded bending moment distributions for test P344 at two different stages of loading : a) at the 1st cycle, and b) at the 6th cycle. The maximum applied load is 960 kN and the minimum load is 0 kN.
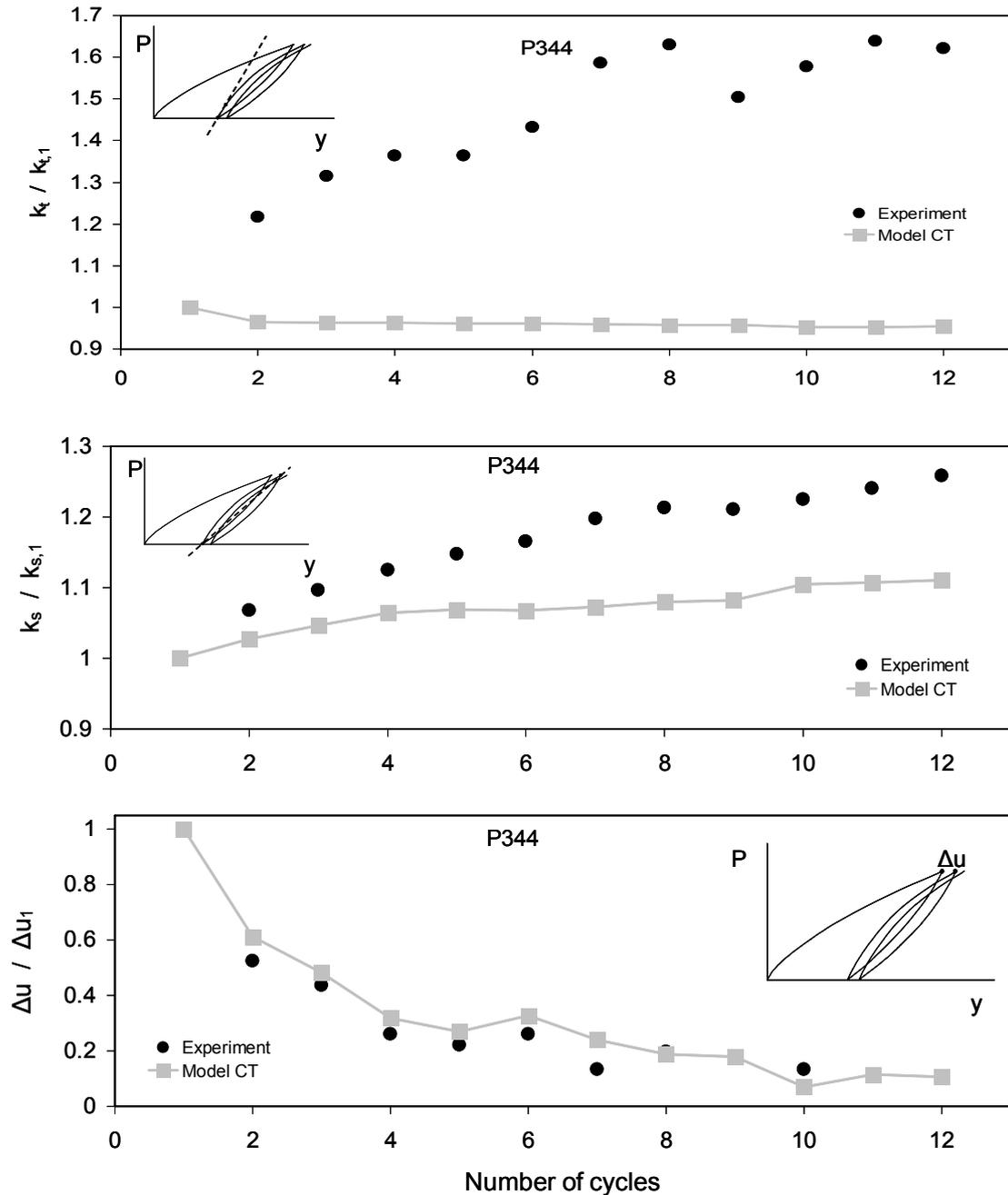
Figure 5. a) Normalized tangent stiffness with respect to the first cycle of loading, b) Normalized secant horizontal pile stiffness with respect to the first cycle of loading, c) Relative pile-head displacement between two consecutive re-loading–unloading reversal points normalized with the one between the loading-unloading and the first re-loading – unloading reversal points

Figure 4 compares the bending moment profiles at the first and sixth cycle of loading. In general, the agreement between the measured and the computed curves is quite satisfactory. The model predicts well the shape of the moment distribution and the increase of the bending moments with the increase of the number of cycles both for loading and unloading of the pile. The model is also capable of simulating the depth of the maximum bending moment both for loading and unloading conditions as well as the shift of the maximum bending moment at a higher depth as the number of cycles increases. The discrepancy in the unloading phase is attributed to that the developed soil constitutive model cannot reproduce soil densification.

Three performance measure parameters where introduced to evaluate the overall response of the pile-soil system. Figure 5a depicts the tangent stiffness at each unloading-reloading reversal point divided by the tangent stiffness at unloading-reloading reversal point of the first cycle, which is indicative of the elastic response of the pile. It is interesting to observe that the computed tangent stiffness remains constant for the proposed model described above, unaffected by cyclic loading, while the measured tangent stiffness increases in test P344. This increase in the measured tangent stiffness is attributed to soil (material) densification during cyclic loading, an effect that is not simulated by the utilized soil constitutive model and which prevails in the elastic response of the pile.

Figure 5b presents the secant stiffness between two sequential reversal points normalized by the secant stiffness of the first cycle, which is indicative of the overall response of the pile during cyclic loading. It is worthy of note that both the computed and the measured secant stiffnesses increase with the number of cycles. Given that the system densification is captured numerically, the difference between measured and computed response is only attributed to soil densification.

Figure 5c presents the relative pile head displacement between two consecutive re-loading–unloading reversal points normalized with the one between the loading-unloading and the first re-loading – unloading reversal points. The pile displacement at pivot points increases in the assymetric cyclic loading with a decreasing rate and the pile finally reaches a zero-plastic strain rate equilibrium. It is observed that the computed versus measured response is in well agreement, implying that the mechanism of "system densification" dominates upon that of soil densification.

4.2 *Simulation of 1x2 pile group*

Having compared and validated the proposed constitutive model with the analysis of a single free-head pile under lateral cyclic loading in nonhomogeneous sand, the effects of lateral cycling loading on a 1x2 pile free-standing free-head pile group are investigated. The piles, located at a distance of three diameters, are parallel to the load direction. The pile heads are hinged (zero bending moment) to the pile cap via appropriate kinematic constraints which ensure the diaphragmatic action towards the loading direction.
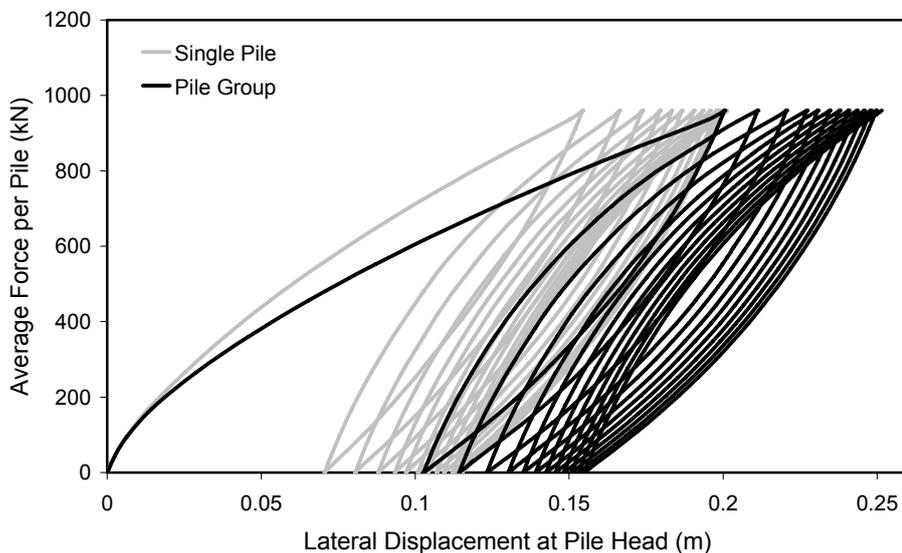
Figure 6. Force – Displacement curve of the single pile and the pile group for the loading of test P344
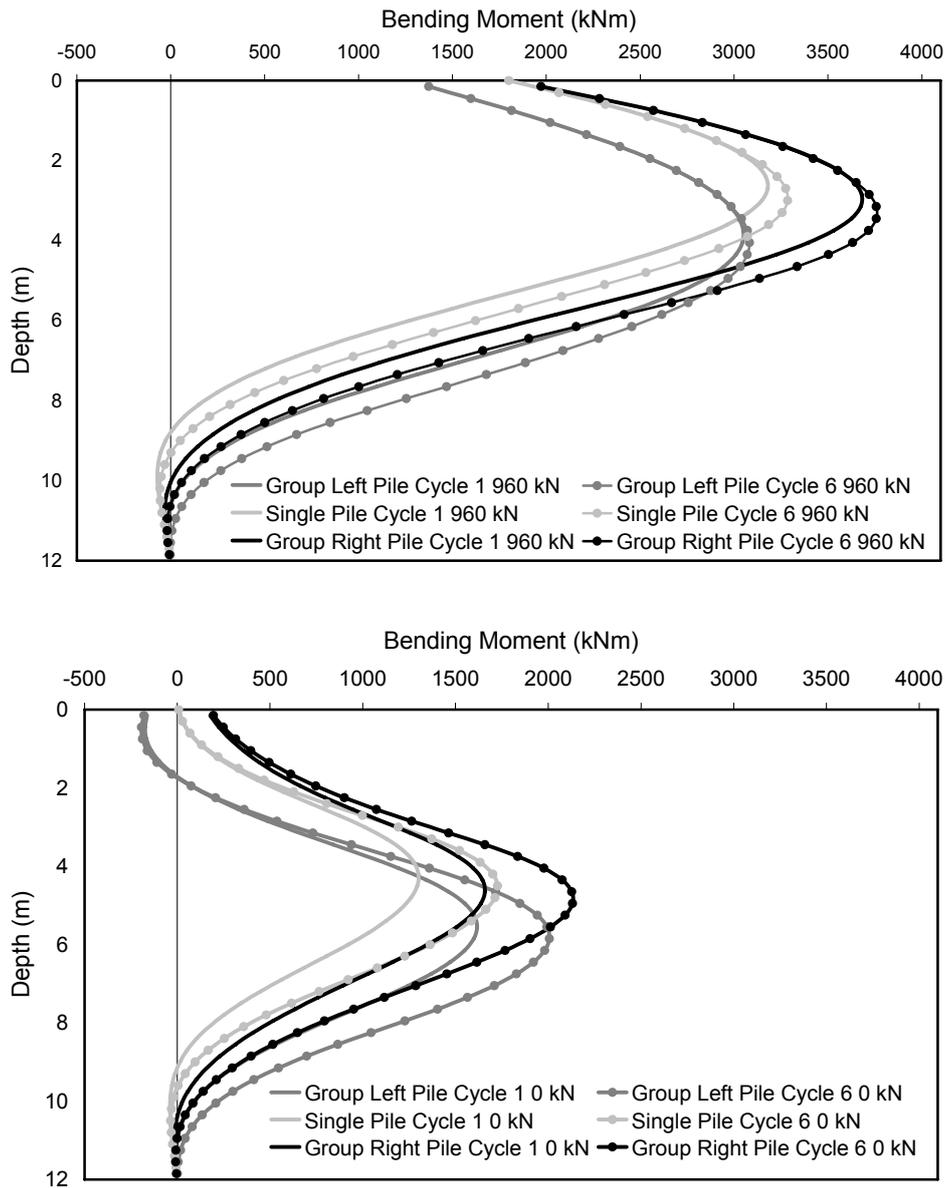
Figure 7. Comparison of computed bending moment distributions of the pile group and the single pile for test P344 at two different stages of loading : a) at the 1st cycle, and b) at the 6th cycle. The maximum applied load is 960 kN and the minimum load is 0 kN.

The pile group is subjected to an asymmetric cyclic lateral loading similar to that of test P344 but with double amplitude (1920 kN). Figure 6 plots the average force per pile versus group displacement and compares it with the corresponding force-displacement loop of the single isolated pile. For the same average load, the group displacement is greater than that of the solitary pile. This behavior is attributed to that the passive failure zones of the piles in the group tend to overlap (shadow effect) as the lateral load increases, thus reducing the average soil resistance on the piles in the group. The shadow effect becomes more dominant with decreasing pile-to-pile distance. As in the case of the free-head single pile, the group displacement increases at a decreasing rate with the number of cycles finally reaching a plastic shakedown equilibrium. Interestingly, the force-displacement loop of the pile group is wider than the corresponding of the single isolated pile, implying greater soil plastification.

Figure 7 depicts the detailed distribution of bending moments with depth along each pile in the group computed for different stages of loading. Comparison is given with the respective re-

sults from the analysis of the single isolated pile. As in the case of the single pile, it is observed that the maximum bending moment increases with the number of cycles and shifts to greater depths following the progressive extension of soil yielding for both piles of the group. Furthermore, the leading pile develops the largest bending moment in comparison to both the trailing and the single pile which shows an intermediate response. The discrepancy in the bending moment distribution between the trailing and the leading pile is attributed to the shadow effect. Finally, upon unloading, and for zero applied lateral force, the bending moments are not zero, instead they retain large values comparable to those for the maximum applied load. This reduction in the maximum values is about 40% for the bending moments. It should be noted, that in the case of a linear soil all the aforementioned quantities would vanish to zero, as soil elasticity would act as a restoring force for the pile.
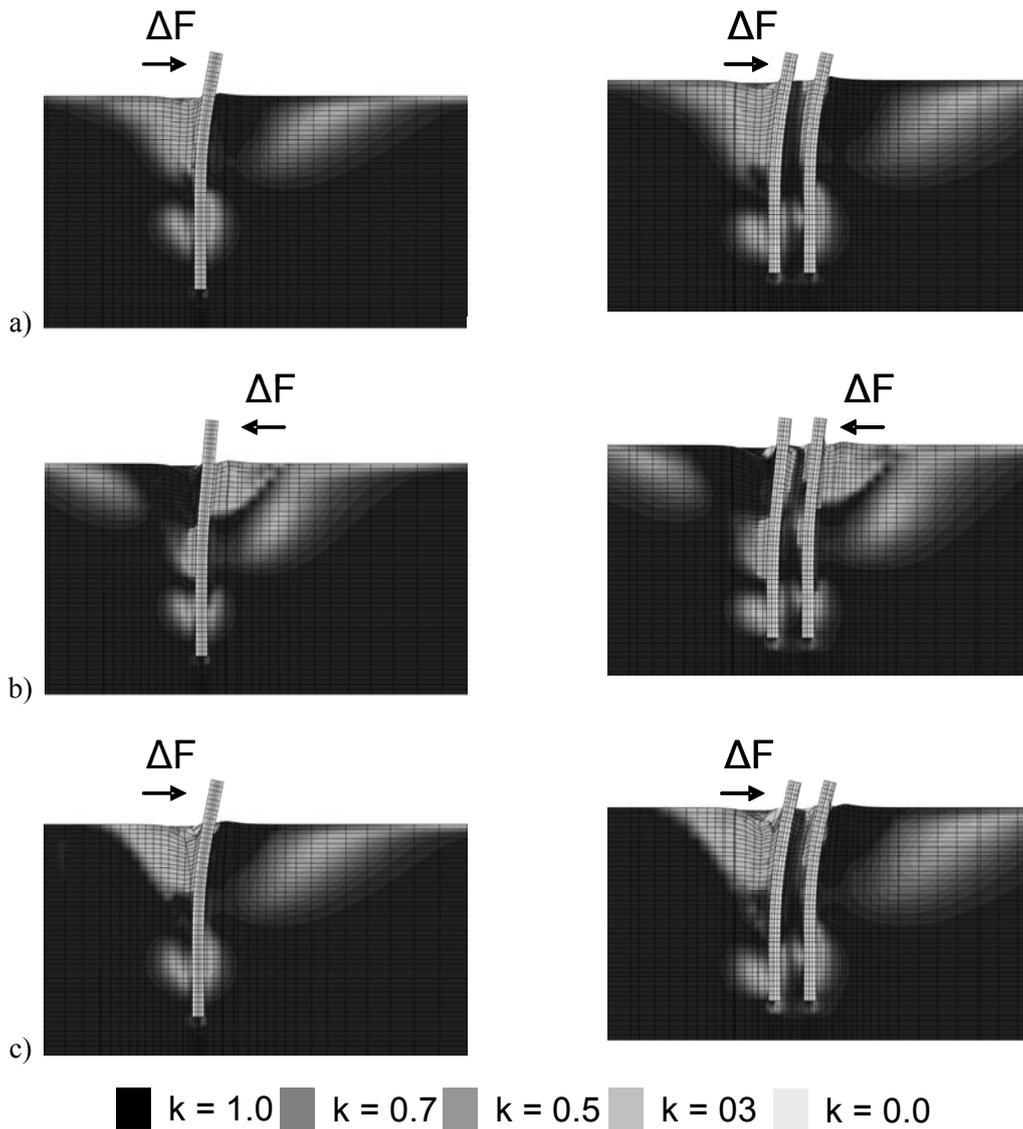
Figure 8. Cross-section of the model with the contours of the active and passive stress states in terms of the state parameter k at three different stages of loading of the single pile and the pile group: a) at the 1st cycle at 960 kN, b) at the 12th cycle at 0 kN, and c) at the 12th cycle at 960 kN. k = 1 corresponds to pure triaxial compression loading condition (passive state), and k = 0 to pure triaxial extension loading condition (active state) while k ≈ 0.5 sets the boundaries between the active and the passive state. (Deformation Scale Factor = 5)

Figure 8 depicts the contours of the active and passive stress states in terms of the state parameter k at three different stages of : a) at the 1st cycle at 960 kN, b) at the 12th cycle at 0 kN, and c) at the 12th cycle at 960 kN for the single pile and the pile group. k = 1 corresponds to pure triaxial compression loading condition (passive state), and k = 0 to pure triaxial extension loading condition (active state) while k ≈ 0.5 sets the boundaries between the active and the passive state. It is interesting to observe that the plastic shakedown effect on the single pile is reflected by the gradually developing fan-shaped stress bulb, the frontal part of which represents the mobilized soil mass that is in a passive state and expands with increasing cycles of loading, while the trailing part corresponds to the mobilized soil zone that is in an active state and shrinks with increasing number of cycles. The larger the bulb of "passive" stresses the greater the lateral soil reactions that resist the applied load, and finally, the pile reaches a steady state equilibrium of constant plastic strain (plastic shakedown). For the case of the pile group, the gradual expansion of the compression stress bulb with number of cycles signals the plastic shakedown process until the pile group reaches a steady state equilibrium of constant plastic strain. The shadow effect is manifested by the formation of a relaxation zone (k = 0) at the back of the leading pile which softens the response of the trailing one.
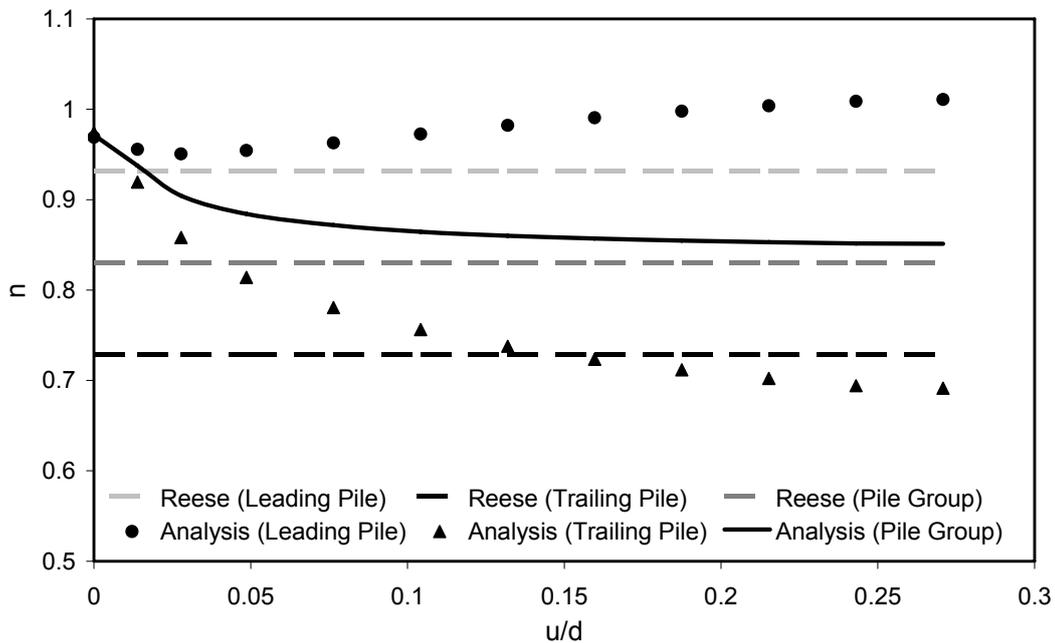
Figure 9. Comparison of efficiency factors of the numerical analysis with the efficiency factors proposed by Reese and Van Impe.

Finally, Figure 9 compares the efficiency factors of the piles (should not be confused with pile-to-pile interaction factors) calculated with the constitutive model and proposed by Reese and Van Impe (2001). It is interesting to observe, that the calculated efficiency factors converge to those of Reese and Van Impe (2001) at very large pile head displacements, with a small discrepancy for the leading pile which shows to recover its initial stiffness ($\eta_l \approx 1$), a hardening response which may be attributed to the plastic shakedown effect. On the contrary, the computed efficiency factor for the trailing pile decreases with increasing horizontal displacement, as a result of the shadow effect, but at decreasing rate due the plastic shakedown induced hardening response of the pile group (reaching a minimum value of ($\eta_t \approx 0.7$).

Of equal, if not more, interest is that at zero and/or very small pile displacements (elastic response), all the three computed efficiency factors (for the leading pile, the trailing pile and the pile group) are very close to 1 (≈ 0.97), implying that pile-to-pile interaction has an insignificant effect on the elastic response of the pile group. This could possibly suggest a "destructive" interference in pile-to-pile interaction rather than that pile-to-pile interaction factors are zero

(which are certainly not, according to valid published results, e.g. Mylonakis and Gazetas 1998). The negligible pile-to-pile interaction effect is also evident in Figure 6 which compares the computed force-displacement response of the single pile and the pile group.

5 CONCLUSIONS

A simplified constitutive soil model for the static and cyclic response of piles embedded in cohesioneless soil was materialized into a three-dimensional finite element code. The model predictions were compared with experimental results of a single pile in dry sand, and subsequently it was applied at a pile group of two piles with similar geometric characteristics and soil conditions to those of the experimental tests. The main conclusions are:
• The plastic shakedown response of both the single pile and the pile group is mostly attributed to the so-called "system" densification rather than to cyclically-induced soil densification.
• During cyclic loading, the mechanism of "system" densification dominates upon soil densification with the contribution of the latter to the macroscopic response of the piles (or pile group) being rather insignificant.
• The formation of a relaxation zone at the back of a leading pile (in the pile group) significantly reduces the lateral soil resistance on the trailing pile. This behavior, well-known in the literature as "shadow effect" is more prominent at large pile deformations.
• The efficiency factor of the leading pile decreases with increasing pile displacement but at extremely large deformations recovers if not overpasses its initial (zero-amplitude) strain value. On the contrary, the efficiency factor of the trailing pile decreases monotonically with loading, but at a decreasing right, finally reaching an asymptotic value.
• The asymptotic values of all three efficiency factors (for the leading pile, the trailing pile and the pile group) compare well with those by Reese and Van Impe, 2001.

6 AKNOWLEDGEMENTS

REFERENCES

Garnier J., 2002, "Properties of soil samples used in centrifuge models", *Invited Keynote Lecture, International Conference on Physical Modelling in Geotechnics – ICPMG '02*, R. Phillips et al. (Eds), published by A.A. Balkema, Rotterdam, 1, pp 5-19.

Gerolymos N., Escoffier S., Gazetas G., Garnier J., 2009, "Numerical Modeling of centrifuge cyclic lateral pile load experiments", *Earthquake Engineering and Engineering Vibration*, 8, pp 61-76

Mylonakis, G. and Gazetas, G. 1998, "Vertical Vibration and Distress of Piles and Pile Groups in Layered Soil", *Soils and Foundations*, Vol. 38, No 1, pp. 1-14

Reese L.C., Van Impe W.F., 2001, Single Piles and Pile Groups under Lateral Loading, *A.A.Balkema*. Rotterdam

Rosquoët F., Garnier J., Thorel L., Canepa Y., 2004, "Horizontal cyclic loading of piles installed in sand : Study of the pile head displacement and maximum bending moment", *Proceedings of the International Conference on Cyclic Behaviour of Soils and Liquefaction Phenomena*, Bochum, T. Triantafyllidis (Ed.), Taylor & Francis, pp 363-368.